Sustainable Hybrid Design to Ensure Efficiency and Air Quality of Solar Air Conditioning

Mohammed Alquraish
Mechanical Engineering Department, College of Engineering, University of Bisha, Saudi Arabia
malqraish@ub.edu.sa (corresponding author)

Khaled Abuhasel
Mechanical Engineering Department, College of Engineering, University of Bisha, Saudi Arabia
kabuhasel@ub.edu.sa

Received: 3 April 2023 | Revised: 29 April 2023 | Accepted: 8 May 2023

 DOI: https://doi.org/10.48084/etasr.5907

ABSTRACT

This research work aims to investigate and subsequently optimize the operating parameters that affect thermal comfort and indoor air quality in the school environment. The proposed design uses a coupling between solar ventilation and the absorption chiller-air conditioning. The heating tower of an adsorption chiller connected to an air conditioning system can be driven by the waste heat from a solar ventilation (exhausted hot air) system thank to this linkage. In order to simulate variables like the velocity magnitude distribution in the air-conditioned room, mathematical modeling is numerically executed. Air temperature evolution along the height of the conditioned room in the mid-length and the air velocity evolution along the length of the conditioned room in the mid-height are studied. According to the numerical simulation results, the inlet air temperature soars as the inlet air velocity rises. Inlet air velocities of 0.05m/s, 0.5m/s, and 1m/s are correlated with inlet air temperatures of 20.7°C, 21.2°C, and 21.3°C, respectively. We conclude that an inlet air velocity in the order of 1m/s (in relation to a maximized air change rate) is in agreement with the general ASHRAE standards for indoor air quality in the case of the school environment, coupled with the essential need to limit as much as possible the spread of viruses.

Keywords-solar air conditioning absorption; ventilation; human comfort

I. INTRODUCTION

The indoor air quality and the thermal comfort in school environment are highly important factors that affect learning and teaching performance. The optimization of such factors within the appropriate standards, will ensure healthy indoor air quality and enhance the human thermal comfort. In this framework, the recent literature reveals some interesting works. Authors in [1] carried out an integrated experimental and simulation approach in order to evaluate the Indoor Environmental Quality (IEQ), principally in terms of acceptable thermal level as well as indoor air quality, under the climate conditions of Florina, Western Macedonia, Greece. Authors in [2] monitored the Indoor Air quality, in terms of air temperature, air relative humidity, CO_2 concentration, $PM_{2.5}$ and PM_{10}, in 10 school classrooms, over a period of one year and under the climate conditions of Victoria, Australia. Results show that the ventilation rates should be increased. Authors in [3] modeled and simulated the effect of wind tower ventilation on classroom thermal comfort during August under the climate conditions of Trabzon, Turkey. The results show that the wind tower ventilation often induces thermal discomfort under the considered climate conditions. Authors in [4] compared different standards to assess the indoor air quality and the thermal comfort in school buildings, under the northern Italy climate conditions. The results show principally that the operative temperature is the most appropriate way to establish and check thermal comfort in classrooms.

The COVID-19 pandemic renewed the interest in indoor air quality and ventilation, in order to limit viruses spreading especially in school environment. Authors in [5] investigated the effects of measures, associated to the COVID-19 pandemic control and prevention, on the ventilation and thermal conditions in 31 Dutch secondary school classrooms. The results show principally that the ventilation rate is enhanced mainly thanks to the occupancy reduction after the COVID-19 lockdown. Also, it was shown that the doors and windows openings were not enough to reach the required ventilation rate. Authors in [6] evaluated the SARS-CoV-2 airborne risk of infection based on natural ventilation rate calculation in an elementary school classroom, under the climate conditions of Uruguay. The results show that periodic ventilation permits to significantly reduce the airborne transmission, even if it is carried out during short time spans.

In the same context, sustainable and hybrid natural ventilation-air conditioning systems are more and more developed to create indoor air quality as well as thermal comfort. Authors in [7] designed a new sustainable hybrid solar ventilation-air conditioning system and investigated its

ventilation and thermal performances under the climate conditions of Gafsa, Tunisia. Technologically speaking, the ventilation is ensured by a solar chimney system while the air conditioning is based on desiccation and adsorption chilling. The coupling between the solar ventilation and the solar air conditioning is based on the use of the wasted heat of the hot air, coming from the outlet of the chimney, to power the heating tower and regenerate the desiccation compartment of the air conditioning system. Authors in [8] proposed a novel natural ventilation design called wind chimney. This design permits to create natural ventilation in buildings located in zones with dominant wind flow, based on aerodynamics law and air pressure difference caused by wind flow. Authors in [9] investigated the impact of the meteorological conditions on the daily incident solar flux on the facades of a house at Adrar region, Algeria. Authors in [10] demonstrated by numerical simulation that the temperature of the internal air varies with climate conditions, location, number of covers, and the solar greenhouse shape. Roofs may be used to generate electricity by connecting PV systems. Authors in [11] studied the solar energy potential and presented an economic study of a 5kW grid-connected rooftop photovoltaic (PV) system in Botswana. Many researchers have proposed hybrid systems for air conditioning, electricity production, and desalination. Authors in [12] presented a solar hybrid system designed for water desalination, air-conditioning, and electricity production.

In Saudi Arabia, individuals are investing more time inside buildings where the utilization of air conditioning is essential. In schools, the chance of disease spreading through bead and vaporized transmission is exceptionally high. Fitting ventilation/air recharging might be a proficient arrangement to decrease infection transmission or other chemical of physical operators delivered by actions (e.g. cooking or smoking) or environment (e.g. sandstorms). It is critical to create advances and consider techniques to handle hyperthermia.

II. SYSTEM DESCRIPTION

The proposed design, shown in Figure 1, uses a coupling between the solar ventilation and the absorption chiller-air conditioning. This coupling permits to recover the waste heat of a solar ventilation (exhausted hot air) system and reuse it to drive the heating tower of an adsorption chiller associated to an air conditioning system. A solar chimney system oriented south is used to ventilate a conditioned space naturally, and an absorption chiller-air conditioning system is used to cool it. In particular, in terms of clothes insulation and air renewal, the suggested design should ensure a person's thermal comfort and a healthy indoor air quality. The air gap is heated by the solar chimney system using the greenhouse effect. This will create a pressure difference that will allow the expelled air from the conditioned room outlet (the solar chimney's inlet (3)) to be driven in the direction of the absorption chiller's heating tower (7-8). The heating tower should be heated and driven by an auxiliary heater AH (6-7) associated with an auxiliary blower AV (5-6) if the heat from the considered ejected air is inadequate to run the heating tower correctly (insufficient solar energy). The absorption chiller can be powered by the cooling and heating towers. The result is the production of the storage of cold water in a cold-water tank, and its use in a water-air radiator (heat exchanger (9)). The blower V1 (1) draws in fresh air (I-Air) from the outside, which is then cooled by the water-air radiator (2). The final step is to inject the obtained process air into the conditioned chamber after being dusted off through the filer F1 (3).

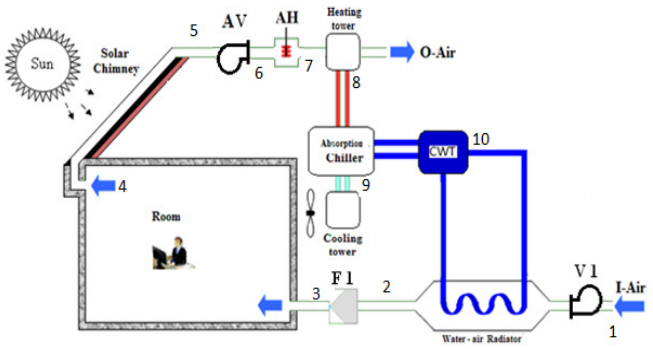

Fig. 1. The proposed solar ventilation-absorption air conditioning system design.

III. MATHEMATICAL MODELING

Special interest is given to the examination of the ventilation and thermal performance of the conditioned area. In this way, the suitable numerical modeling is based on the Navier-Stokes conditions in terms of progression condition, x and y-momentums conditions, vitality preservation condition as well as turbulent dynamic vitality and turbulent scattering [4]. The heat exchange model is considered in bi-dimensional steady state with the k-ε turbulence model. The Boussinesq estimation is expected since the air temperature contrast between solar chimney inlet and outlet is considered low.

A. Continuity Equation

The continuity equation reflects the principle of mass conservation in terms of relation between the air velocity and the cross-sectional area through which the fluid flows. The decrease of this cross-sectional area induces an increase of air velocity. The continuity equation is written as:

$$\frac{\partial u}{\partial x}+\frac{\partial v}{\partial y}=0 \quad (1)$$

B. Momentum Equations

The momentum equations reflect the principle of linear momentum conservation along a specific direction in space. The momentum of an object is the product of its mass and its linear velocity. It represents the quantity of motion of the considered object. The momentum equations along the x- and y-directions of the space are written as:

$$\frac{\partial uu}{\partial x}+\frac{\partial vu}{\partial y}=-\frac{1}{\rho}\frac{\partial}{\partial x}\left((\mu+\mu_t)\frac{\partial u}{\partial x}\right)+\frac{1}{\rho}\frac{\partial}{\partial y}\left((\mu+\mu_t)\frac{\partial u}{\partial y}\right)-\frac{2}{3}\frac{\partial k}{\partial x} \quad (2)$$

$$\frac{\partial uv}{\partial x}+\frac{\partial vv}{\partial y}=-\frac{1}{\rho}\frac{\partial P}{\partial y}+\frac{1}{\rho}\frac{\partial}{\partial x}\left((\mu+\mu_t)\frac{\partial v}{\partial x}\right)$$
$$+\frac{1}{\rho}\frac{\partial}{\partial y}\left((\mu+\mu_t)\frac{\partial v}{\partial y}\right)-\frac{2}{3}\frac{\partial k}{\partial x}+g\beta(T-T_0) \quad (3)$$

C. Energy Conservation Equation

As its name suggests, this equation reflects the principle of energy conservation. It expresses the first law of thermodynamics as a balance equation for the rate of change of kinetic energy and internal energy. The energy conservation equation is written as:

$$\frac{\partial uT}{\partial x}+\frac{\partial vT}{\partial y}=\frac{1}{\rho}\frac{\partial}{\partial x}\left(\left(\frac{\mu}{\mathrm{Pr}}+\frac{\mu_t}{\mathrm{Pr}_t}\right)\frac{\partial T}{\partial x}\right)$$
$$+\frac{1}{\rho}\frac{\partial}{\partial y}\left(\left(\frac{\mu}{\mathrm{Pr}}+\frac{\mu_t}{\mathrm{Pr}_t}\right)\frac{\partial T}{\partial y}\right) \quad (4)$$

D. Turbulent Kinetic Energy

The turbulent kinetic energy k reflects the intensity of turbulence in a flow. The equation governing the transport of the turbulent kinetic energy k is written as:

$$\frac{\partial uk}{\partial x}+\frac{\partial vk}{\partial y}=\frac{1}{\rho}\frac{\partial}{\partial x}\left(\left(\mu+\frac{\mu_k}{\mathrm{Pr}_k}\right)\frac{\partial K}{\partial x}\right)$$
$$+\frac{1}{\rho}\frac{\partial}{\partial y}\left(\left(\mu+\frac{\mu_k}{\mathrm{Pr}_k}\right)\frac{\partial k}{\partial y}\right)+\frac{1}{\rho}(G_k+G_b)-\varepsilon \quad (5)$$

E. Turbulence Dissipation

The turbulent dissipation reflects the viscous conversion of mechanical energy to heat. The equation governing the turbulence dissipation ε is written as:

$$\frac{\partial u\varepsilon}{\partial x}+\frac{\partial v\varepsilon}{\partial y}=\frac{1}{\rho}\frac{\partial}{\partial x}\left(\left(\mu+\frac{\mu_t}{\mathrm{Pr}_t}\right)\frac{\partial \varepsilon}{\partial x}\right)$$
$$+\frac{1}{\rho}\frac{\partial}{\partial y}\left(\left(\mu+\frac{\mu_t}{\mathrm{Pr}_t}\right)\frac{\partial \varepsilon}{\partial y}\right)+C_{1\varepsilon}\frac{\varepsilon}{\rho k}\frac{1}{\rho}(G_k+C_{3\varepsilon}G_b) \quad (9)$$
$$-C_{2\varepsilon}\frac{\varepsilon^2}{k}$$

where the empirical constants $C_{1\varepsilon}$, $C_{2\varepsilon}$ and $C_{3\varepsilon}$ have the values of 1.44, 1.92, and 0.09, respectively, $\mathrm{Pr_k}$ and $\mathrm{Pr_\varepsilon}$, are the turbulent Prandtl numbers for the variables k and ε having values of 1.0 and 1.3, respectively, and G_k indicates the gradients in mean velocity:

$$G_k=\mu_t\left(\frac{\partial u_i}{\partial x_j}+\frac{\partial u_j}{\partial x_i}\right)\frac{\partial u_i}{\partial x_j}-\frac{2}{3}\rho k\delta_{ij}\frac{\partial u_i}{\partial x_j} \quad (7)$$

G_b represents the production of the turbulent kinetic energy due to the buoyancy:

$$G_b=\beta g_i\frac{\mu_t}{\mathrm{Pr}_t}\frac{\partial T}{\partial x_i} \quad (8)$$

It can be concluded that the mathematical modeling governing the ventilation and the thermal performance of the conditioned area was elaborated under the assumptions of Boussinesq approximation as well as the bi-dimensional steady state heat transfer with the k-ε turbulence model. In the next section, this mathematical modeling is numerically implemented. The simulation results are presented and discussed.

IV. RESULTS

A. Air Flow within the Conditioned Room

Figure 2 shows the air velocity magnitude distribution within a conditioned room with length X=4m and height H=3m. The inlet of the air is located to the lower right wall, while the outlet air is connected to the inlet of the solar chimney and it is located in the top of left wall. The inlet air velocity is varied as 0.05m/s, 0.5m/s, and 1m/s. It is clear that the air breeze (forced air flow) carried out between the air inlet and the outlet keeps almost the same shape with a global air velocity enhancement as the inlet air velocity increases. The global air velocity distribution above the air breeze is slightly more pronounced than that below. This is expected since the space occupied by the air above the air breeze is significantly larger than that below. It should be also noted that the air velocity magnitude in the neighborhood of the air outlet is enhanced. This is expected since the air outlet is connected to the solar chimney inlet where a strong air suction effect is applied.

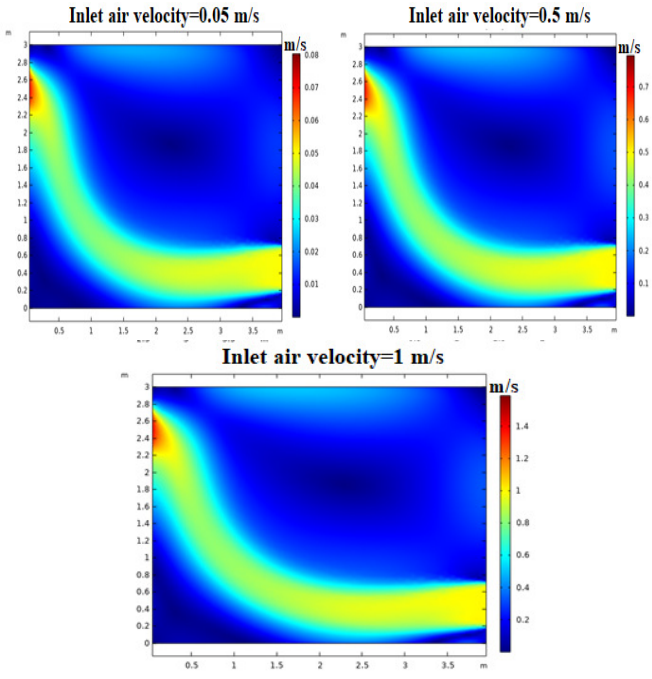

Fig. 2. Air velocity magnitude distribution in the conditioned room.

Figure 3 depicts the vertical evolution of the air velocity along the height of the conditioned room in the mid-length level defined by x=2m. The inlet air velocity is 1m/s, 0.5m/s, and 0.05m/s. The room air velocity rapidly increases from 0.26m/s, 0.14m/s, and 0.02m/s to reach a maxima in the neighborhood of h=0.7m of 0.91m/s, 0.45m/s, and 0.05m/s for an inlet air velocity in the order of 1m/s, 0.5m/s, and 0.05m/s, respectively. This is expected since the air velocity in this room region (room bottom) is highly influenced by the air breeze carried out between the air inlet and outlet of the conditioned room. Between h=0.7m and h=1.45m, the room air velocity rapidly decreases to 0.3m/s, 0.15m/s, and 0.05m/s for an inlet air velocity of 1m/s, 0.5m/s and 0.05m/s respectively. Between h=1.45m and h=2.6m, the room air velocity moderately decreases to 0.04m/s, 0.02m/s, and 0.005m/s for an inlet air velocity in the order of 1m/s, 0.5m/s, and 0.05m/s, respectively. This is expected since this room region is relatively far from the influence of the air. Between h=2.6m and h=3m, the room air velocity moderately increases to reach 0.12m/s, 0.06m/s, and 0.01m/s for an inlet air velocity of 1m/s, 0.5m/s, and 0.05m/s respectively. This is expected since this room region is close to the inlet of the solar chimney (located in the top region of the room) where the air velocity is more pronounced due to the strong suction effect induced by the solar chimney. It should be noted that the air velocity increase and decrease rates are more pronounced for higher inlet air velocity.

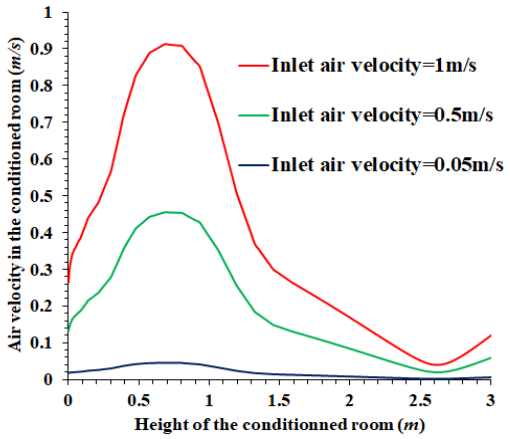

Fig. 3. Air velocity evolution along the height of the conditioned room in the mid-length.

B. Air Temperature in the Conditioned Room

Figure 4 depicts the horizontal evolution of the air temperature along the length of the conditioned room in the mid-height level defined by h=1.5m. The inlet air velocity is varied as 0.05m/s, 0.5m/s, and 1m/s. The room air temperature rapidly decreases from 21.8°C, 22.4°C, and 22.45°C to a minimum in the neighborhood of x=0.5m (left side of the room) of 17.2°C, 17.1°C, and 17.1°C, for an inlet air velocity of 0.05m/s, 0.5m/s, and 1m/s, respectively. Between x=0.5m and x=1.1m, the room air temperature evolutions rapidly increase to 18.4°C, 18°C and 17.9°C for inlet air velocity of 0.05m/s, 0.5m/s, and 1m/s respectively. This important increase and decrease rates are expected since the convection in this room region (close to the inlet of the solar chimney) is enhanced by the pronounced air velocity caused by the strong suction effect induced by the solar chimney. Between x=1.1m and x=3.5m, the room air temperature evolutions stagnate around 18.3°C, 17.9°C, and 17.8°C for an inlet air velocity in the order of 0.05m/s, 0.5m/s, and 1m/s, respectively. Between x=3.5m and x=4m, the room air temperature drastically increases to 20.7°C, 21.2°C, and 21.3°C for inlet air velocity of 0.05m/s, 0.5m/s, and 1m/s, respectively. It should be noted that the air velocity increase and decrease rates are more pronounced for higher inlet air velocity.

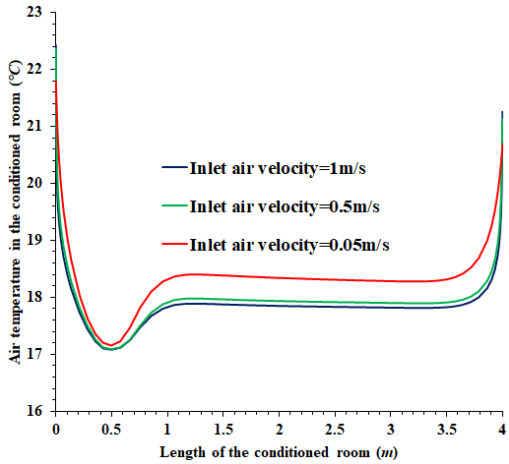

Fig. 4. Air temperature evolution along the length of the conditioned room at the mid-height.

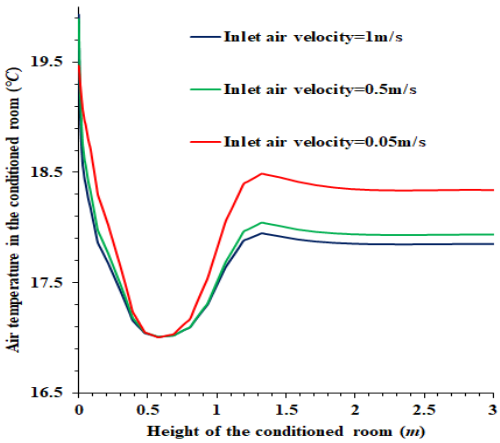

Fig. 5. Air temperature evolution along the height of the conditioned room in the mid-length.

Figure 5 depicts the vertical evolution of the air temperature along the height of the conditioned room in the mid-length level defined by x=2m. The inlet air velocity is varied as 0.05m/s, 0.5m/s, and 1m/s. The room air temperature rapidly decreases from 19.47°C, 19.89°C, and 19.93°C to reach a minimum in the neighborhood of h=0.6m (left side of the room) in the order of 17.0°C for all inlet air velocity values. Between x=0.6m and x=1.35m, the room air temperature rapidly increases to 18.5°C, 18.1°C, and 17.95°C for inlet air

velocity of 0.05m/s, 0.5m/s, and 1m/s, respectively. It is to note that the air velocity increase and decrease rates are slightly more pronounced for higher inlet air velocity values. These increase and decrease rates are expected since the convection in this room region (located in the bottom side of the room) is highly influenced by the air breeze carried out between the air inlet and outlet of the conditioned room. Between h=1.35m and h=3m, the room air temperature stagnates around 18.35°C, 17.95°C, and 17.85°C for inlet air velocity of 0.05m/s, 0.5m/s, and 1m/s, respectively.

C. *Thermal Comfort and Indoor Air Quality*

The proposed design ensures two tasks:

- Acceptable thermal comfort in a school environment.
- Acceptable indoor air quality in a school environment.

The comfort zone is within the air temperature range from 18°C to 27°C while the air relative humidity range is from 20% to 80% with a slight air temperature limitation from 28°C to 25°C when the relative humidity passes from 50% to 80%. Taking into account the morning air relative humidity in the region of Bisha, Saudi Arabia in May and June (globally around 47% and 29%, respectively), it is easy to locate the (inlet air temperature, inlet air relative humidity) points on the psychrometric chart. Figure 6 shows that the inlet air is within the thermal comfort zone for both May and June.

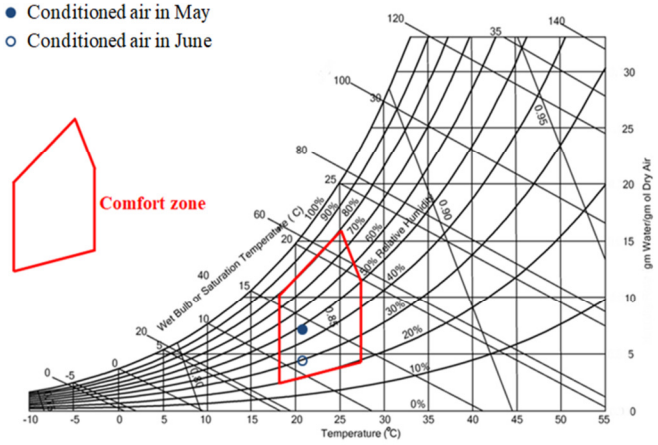

Fig. 6. Inlet air within the comfort zone in May and June.

V. DISCUSSION AND OPTIMIZATION OF AIR CONDITIONING PARAMETERS

In this paper, the two major air-conditioning parameters, inlet air temperature and inlet air velocity, are optimized with the goal of improving thermal comfort and indoor air quality in the school environment. The air-conditioning optimization should ensure a compromise between appropriate inlet air temperature and inlet air velocity, inducing the highest possible air change rate and the lowest possible air temperature, while remaining within the limits of human thermal comfort.

According to the results of numerical simulations, the inlet air temperature rises as the inlet air velocity rises (this is directly related to the air change rate). Inlet air temperatures in the order of 20.7°C, 21.2°C, and 21.3°C are associated to inlet air velocities in the order of 0.05m/s, 0.5m/s, and 1m/s, respectively. The inlet air velocity in the range of 0.05m/s is disallowed within the parameters of the optimization under consideration because it causes stagnation, which significantly worsens thermal comfort and raises the risk of virus transmission. Thus, an inlet air velocity in the order of 0.5m/s that is associated to the lowest inlet air temperature (21.2°C), shall be selected as a primary choice. However, the inlet air temperature associated to an inlet air velocity of 1m/s is in the order of 21.3°C. So, it is clear that there is no perceptible air temperature difference when the inlet air velocity passes from 0.5m/s to 1m/s. It is appropriate to choose, as the final optimization step, an inlet air velocity in the order of 1m/s associated with an inlet air temperature in the order of 21.3°C because the air change rate should be maximized as much as possible. The general ASHRAE standards [13] for indoor air quality in the case of a school environment, along with the crucial need to limit the spread of viruses as much as possible, are in agreement with an inlet air velocity in the order of 1m/s (in relation with a maximized air change rate).

VI. CONCLUSION

The ability to create thermal comfort in the conditioned area and its thermal performance are numerically investigated, presented, and discussed in this paper. It is appropriate to select an inlet air velocity of 1m/s and an inlet air temperature of 21.3°C because the air change rate should be increased as much as possible in the school environment to prevent virus spreading. Future research on the hybrid solar ventilation-air conditioning design is conceivable, with the goal of enhancing its ventilation, hygrometric, and thermal performance along with its sustainability in relation to the use of solar energy. Also, a desiccant compartment can be integrated and investigated in order to improve the hygrometric and thermal capacities of the considered air-conditioning system. It should be noted that an appropriate coupling between the solar ventilation system and the desiccant compartment can be studied in the future.

ACKNOWLEDGMENT

The authors are thankful to the Deanship of Scientific Research at University of Bisha for the financial support.

REFERENCES

[1] G. Papadopoulos, "IEQ assessment in free-running university classrooms," *Science and Technology for the Built Environment:*, vol. 28, no. 7, pp. 823–842, https://doi.org/10.1080/23744731.2022.2052519.

[2] P. Rajagopalan, M. A. Andamon, and J. Woo, "Full article: Year long monitoring of indoor air quality and ventilation in school classrooms in Victoria, Australia," *Architectural Science Review*, vol. 65, no. 1, pp. 1–13, Oct. 2021, https://doi.org/10.1080/00038628.2021.1988892.

[3] R. Rabeharivelo, M. Kavraz, and C. Aygün, "Thermal comfort in classrooms considering a traditional wind tower in Trabzon through simulation," *Building Simulation*, vol. 15, pp. 401–418, 2022, https://doi.org/10.1007/s12273-021-0804-9.

[4] F. Babich, G. Torriani, J. Corona, and I. Lara-Ibeas, "Comparison of indoor air quality and thermal comfort standards and variations in exceedance for school buildings," *Journal of Building Engineering*, vol. 71, Jul. 2023, Art. no. 106405, https://doi.org/10.1016/j.jobe.2023.106405.

[5] E. Ding *et al.*, "Ventilation and thermal conditions in secondary schools in the Netherlands: Effects of COVID-19 pandemic control and prevention measures," *Building and Environment*, vol. 229, Feb. 2023, Art. no. 109922, https://doi.org/10.1016/j.buildenv.2022.109922.

[6] A. Vignolo, A. P. Gómez, M. Draper, and M. Mendina, "Quantitative Assessment of Natural Ventilation in an Elementary School Classroom in the Context of COVID-19 and Its Impact in Airborne Transmission," *Applied Sciences*, vol. 12, no. 18, Jan. 2022, Art. no. 9261, https://doi.org/10.3390/app12189261.

[7] F. Nasri, F. Alqurashi, R. Nciri, and C. Ali, "Design and simulation of a novel solar air-conditioning system coupled with solar chimney," *Sustainable Cities and Society*, vol. 40, pp. 667–676, Jul. 2018, https://doi.org/10.1016/j.scs.2018.04.012.

[8] J. Shaeri, M. Mahdavinejad, and M. H. Pourghasemian, "A new design to create natural ventilation in buildings: Wind chimney," *Journal of Building Engineering*, vol. 59, Nov. 2022, Art. no. 105041, https://doi.org/10.1016/j.jobe.2022.105041.

[9] A. Oudrane, B. Aour, B. Zeghmati, X. Chesneau, and H. Massaoud, "Study and Simulation of the Density of the Incident Solar Flux on the Walls of a Building in Adrar, Algeria," *Engineering, Technology & Applied Science Research*, vol. 7, no. 5, pp. 1940–1945, Oct. 2017, https://doi.org/10.48084/etasr.1337.

[10] J. Yau, J. J. Wei, H. Wang, O. Eniola, and F. P. Ibitoye, "Modeling of the Internal Temperature for an Energy Saving Chinese Solar Greenhouse," *Engineering, Technology & Applied Science Research*, vol. 10, no. 5, pp. 6276–6281, Oct. 2020, https://doi.org/10.48084/etasr.3728.

[11] Y. Kassem, H. Gokcekus, and F. A. R. Agila, "Techno-Economic Feasibility Assessment for the promotion of Grid-Connected Rooftop PV Systems in Botswana: A Case Study," *Engineering, Technology & Applied Science Research*, vol. 13, no. 2, pp. 10328–10337, Apr. 2023, https://doi.org/10.48084/etasr.5668.

[12] A. Fouda, H. Elattar, S. Rubaiee, A. S. B. Mahfouz, and A. M. Alharbi, "Thermodynamic and Performance Assessment of an Innovative Solar-Assisted Tri-Generation System for Water Desalination, Air-Conditioning, and Power Generation," *Engineering, Technology & Applied Science Research*, vol. 12, no. 5, pp. 9316–9328, Oct. 2022, https://doi.org/10.48084/etasr.5237.

[13] *2016 ASHRAE Handbook—HVAC Systems and Equipment*. ASHRAE, 2008.